Resilience of QPSK Radio Links Under Narrowband and Broadband Electromagnetic Interferences

ASIF ALI[1], MIREYA FERNÁNDEZ CHIMENO[1], AND MARCO A. AZPÚRUA[1,2] (Senior Member, IEEE)

[1]Grup de Compatibilitat Electromagnètica, Universitat Politècnica de Catalunya, 08034 Barcelona, Spain

[2]EMC Electromagnetic BCN, S.L EMC Barcelona, 08034 Barcelona, Spain

CORRESPONDING AUTHOR: A. ALI (e-mail: asif.ali@upc.edu)

ABSTRACT Electromagnetic interference has the potential to affect the functionality and performance of radio communication links. This work investigates the impact electromagnetic disturbances have on such wireless links, taking quadrature phase-shift keying (QPSK) as a representative example. The evaluation of the effects of interference on a QPSK radio link becomes relevant as it is used by the IEEE 802.11b protocol. Through simulations, we study a QPSK link subjected to narrowband and broadband disturbances. The bit error rate (BER) and the error vector magnitude (EVM) are our quality assessment metrics for evaluating the system. Two specific scenarios are analyzed: continuous wave and chirp interferences as in-band and out-band conditions. The results indicate that the applied electromagnetic interference can degrade the signal quality, resulting in high BER. Furthermore, it is observed that chirp interference largely affects the radio links more than continuous wave disturbances. The aforementioned findings support and reinforce the applicability of the analysis methodology in real-life scenarios like those characterizing healthcare settings.

INDEX TERMS Communication quality, electromagnetic compatibility, electromagnetic interference, electromagnetic resilience.

I. INTRODUCTION

IN LIGHT of the increasing need for enhanced data rates and reliable communication, it is crucial to understand the radio link quality and communication metrics within the context of electromagnetic compatibility (EMC). EMC plays an essential role in controlling and minimizing interferences to communication links so electromagnetic disturbances from other systems or external sources do not disrupt wired or wireless signals [1]. It is well known that electromagnetic interference (EMI) can reduce the effectiveness of wireless radio links [2], [3]. Therefore, it is critical to optimize the resilience to EMI of digital links so that their performance is improved [4]. Therefore, the capacity of the system to withstand and operate efficiently in the presence of EMI is a factor to consider when assessing the resilience of a radio communication link.

This study aims to examine the utilization of quadrature phase shift keying (QPSK) modulation in a harsh electromagnetic scenario. QPSK is a robust modulation technique to transmit more data with the same bandwidth, and it is less sensitive to noise and interference [5] with respect to other modulation schemes such as binary phase shift keying. Investigating the EMI resilience of QPSK is important because of its many applications in medical devices. For example, it is utilized in biomedical implanted devices to facilitate wireless communication between internal and external components [6]. Another application is the battery-less ASK/O-QPSK transmitter designed for medical implants [7]. Furthermore, [8], [9] describes a low-power multichannel transmitter that utilizes binary frequency shift keying and QPSK modulation techniques for wireless bio-telemetry devices.

The EMI challenges discussed in the studies [10], [11], [12] are crucial to identify useful solutions that can minimize the interference in digital communication systems (DCS). Their research focuses on employing

interference cancelation techniques to improve DCS performance in EMI-prone environments. We emphasize the importance of conducting a comprehensive analysis of the environment, considering communication protocols, frequencies, and power levels while evaluating interference sources. The evaluation of radio link resilience to interference in terms of SNR, and BER [13] is relevant to our work. Previous studies [14], [15], [16] placed significant emphasis on the effect of interference frequencies and pulse parameters on the BER of the radio link. Moreover, EMI from modular multilevel converter submodules that produce voltage and current transients can have an impact on wireless communication. In [17], researchers test the impact of EMI on wireless communication in the multi-GHz frequency spectrum. Sub-500 MHz component interference has less influence on wireless communication at the 5825 MHz central frequency.

However, these studies often overlook the influence of different EMI levels and multiple interferences. Our research aims to bridge this gap by considering these factors. Interferences from external sources, including continuous waves (CW) and chirps, have a negative impact on the communication link performance. CW interference is caused by the presence of a single frequency or narrowband signal in the vicinity of the system [18], while chirp signals are intermittent signals that increase or decrease in frequency over time [19]. Jammers can cause broadband EMI by producing noisy signals that mislead nearby devices with the same frequency, disrupting communications.

As an example, the disturbance voltage at the GPS receiver due to a jammer was measured in our laboratory, and these measurements reflect an appearance of chirp interference, as illustrated in Fig. 1. The interference of these signals can cause various problems, such as signal fading, loss of bandwidth, and degradation of signal quality [20]. The goal of this study is to assess the performance of the digital radio link in the presence of both CW and chirp interferences.

A. MAIN CONTRIBUTIONS
The primary contributions of this study are:
- An effective simulation model for the evaluation of QPSK radio links is presented. It offers a methodology, which is novel in the EMC domain, for assessing the digital link efficiency in the presence of CW and chirp EMI.
- The study examines two separate EMI scenarios, namely in-band and out-of-band, in order to conduct a thorough evaluation of baseband QPSK radio links.

The paper structure is as follows: Section II of the paper discusses the types of EMI considered in this study. Section III provides an explanation of the proposed approach for assessing radio link performance in EM environments in relation to the interference. Section IV of the work presents a comprehensive analysis of the simulation results, while Section V serves as the concluding section, summarizing the key findings and implications of the study.
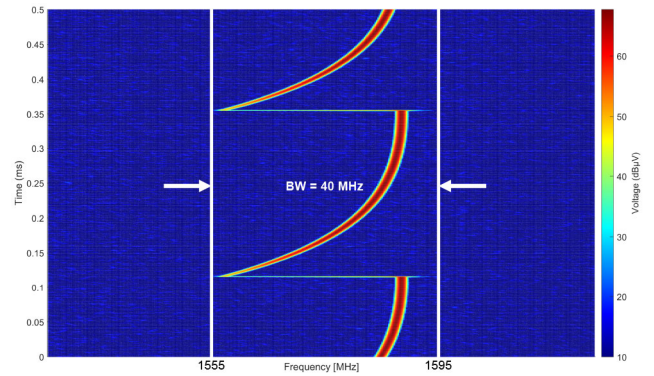

FIGURE 1. Example of a source of intentional EMI. Spectrum of the measured disturbance voltage produced by a GPS jammer at the receiver antenna port.

II. EMI IN COMMUNICATION LINKS
EMI arises from both natural and man-made sources, resulting in disturbances in the functionality of electronic devices and communication links [21]. Even though EMI is usually unintentional, it can be considered similarly to co-channel and adjacent channel interferences, depending on whether the EMI spectrum is in-band or out-of-band. EMI control and mitigation are commonly carried out following what has been called the "rule-based approach", that is following a structured, often standard, procedure to identify and mitigate EMI.

However, the rule-based approach has limitations for EMI control on DCS due to their dynamic and constantly changing characteristics. The complexities inherent in digital systems surpass the limitations of rule-based approaches, hence emphasizing the necessity for more comprehensive frameworks established based on fundamental principles. As a first step to improve the EMI assessment, the different influences of narrowband and broadband EMI shall be analyzed.

A. NARROWBAND EMI
CW signals are a subset of narrowband signals because they have only one spectral line that falls within the passband of an intermediate frequency filter. The primary source of narrowband EMI are harmonics of high-speed digital signals and fast switching of power electronics.

B. BROADBAND EMI
A chirp is a signal whose frequency increases or decreases over time and it is a representative example of broadband EMI. It is commonly used in spread-spectrum applications [22]. The linear chirp expression is (1), where ϕ_0 is the phase of the chirp, f_0 is the start frequency ($t = 0$) and c is the chirp rate defined as the frequency variation divided by the sweep time, as given by,

$$x(t) = \sin\left[2\pi\left(\frac{c}{2}t^2 + f_0 t\right) + \phi_0\right]. \qquad (1)$$
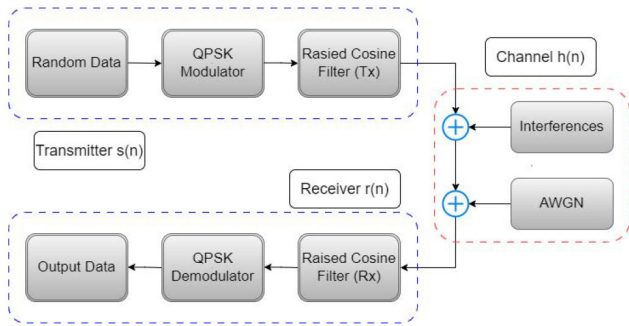
FIGURE 2. QPSK radio link block diagram for simulation.

TABLE 1. Simulation parameters to create the QPSK radio link.

Parameters	Values
Sample rate	2 MHz
Modulation order	4
Tx bits	120 kbits
Roll of factor	0.3
Filter span	10
In and out samples per frame	4
SNIR	-15 dB to 15 dB
Continuous EMI	500 kHz and 2 MHz
Initial frequency of chirp	0 Hz
Chirp EMI	500 kHz and 2 MHz
Chirp duration	1 ms

III. METHODOLOGY

Simulations were run using the MATLAB Communications Toolbox to model the radio link performance in the face of the EMI types defined in the scope. The assessment is based on predetermined performance quality metrics. The methodology will be explained in its three main steps: system model, communication quality metrics, and system validation.

A. SYSTEM MODEL

Fig. 2 depicts the system model employed to establish the radio communication link. This model simulates a DCS and evaluate performance employing two distinct kinds of interference. It consists of three primary components, namely a transmitter, a receiver, and a channel where interference is introduced.

To build the transmitter, it is necessary to include a random data generator, a QPSK modulator, and a raised cosine transmitter filter. At the receiver end, we employ a QPSK demodulator in conjunction with a raised cosine receiver filter to process the incoming signal. The resulting output data is then obtained. The interferences and the white noise are added to the channel. Table 1 displays the parameters configured for the simulation of the DCS and these parameters were identified via the trial and error method. In this case, the computational complexity is not a crucial consideration. We carried out simulations using a standard PC equipped with basic tools. In addition, the current implementation uses fixed parameters and no adaptive features are simulated.

This MATLAB simulation presents how to construct a QPSK transmitter for digital communication links. QPSK modulates the signal phase to encode digital data. The code generates a suitable random binary input sequence of 120 kbits and sets QPSK modulation order to 4. After translating binary input into symbols and applying QPSK modulation with a phase offset, the code shapes the waveform using a raised cosine transmit filter and adjusts the sample rate. This simulation is crucial to demonstrating digital communication link QPSK transmitter operation. The simulation emphasizes baseband radio bandwidth preservation through filter choices, including a roll-off factor of 0.3.

The filter span restricts the number of symbols that are processed, taking into account an impulse response that has been truncated to 4 symbols, which is also important in signal processing.

The signal, in the presence of interference, is transmitted through an additive white gaussian noise (AWGN) channel in order to simulate the impact of noise within a communication system as mentioned in the flowchart (Fig. 3). The signal-to-noise-and-interference ratio (SNIR) is a crucial figure in this particular situation. It enables the control of interference and noise levels according to specific needs, hence imposing practical limitations on the signal.

The QPSK receiver in the digital system processes the incoming signal to achieve optimal performance. The process begins with the signal being subjected to shaping and filtering via a raised cosine receive filter, which serves a dual purpose. Subsequently, the filtered signal undergoes demodulation utilizing QPSK demodulation techniques. The assessment of system performance under different SNIR levels is contingent upon the computation of the BER, which involves the comparison of the demodulated symbols to the initially transmitted symbols.

B. COMMUNICATION QUALITY METRICS

In this study, the quality metrics employed for assessing the resilience of QPSK radio links to EMI are the bit error rate (BER) and the error vector magnitude (EVM). The BER refers to the number of bits within a data stream that have undergone alteration due to factors such as noise, interference, distortion, or issues pertaining to bit synchronization. BER represents the rate of bit errors to the total number of transferred bits within a specified time interval. EVM quantifies the extent to which points deviate from their optimal locations, thereby serving as an indicator of the precision of the system as defined by (2), where X_{error} is the absolute value of error and $X_{reference}$ is the expected value or reference value to compare your measurements

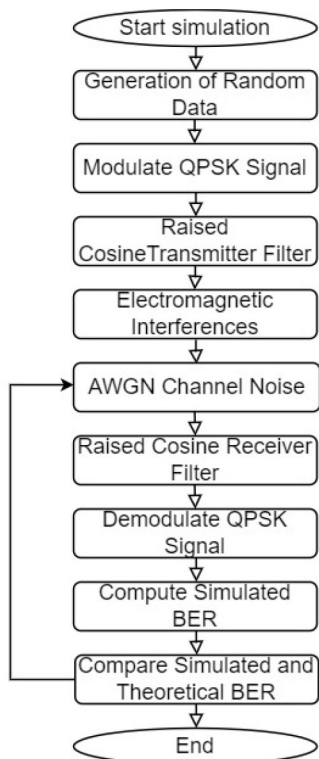$$EVM(\%) = \frac{X_{error}}{X_{reference}} \cdot 100\%. \quad (2)$$
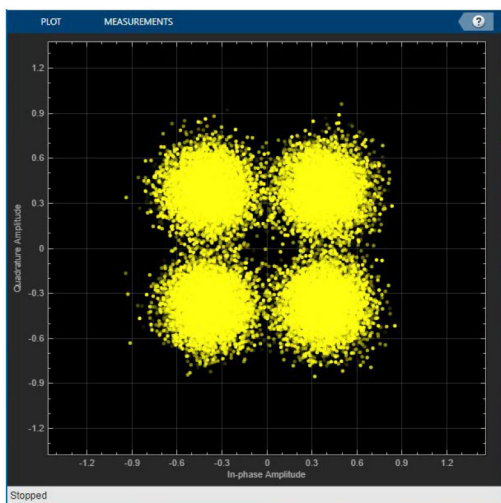
2393

FIGURE 3. QPSK radio link flowchart to perform simulation.

FIGURE 4. QPSK radio link constellation diagram symbols showed an SNIR power level of 15 dB without intentional EMI injection.

FIGURE 5. Validation. QPSK signal waveform.
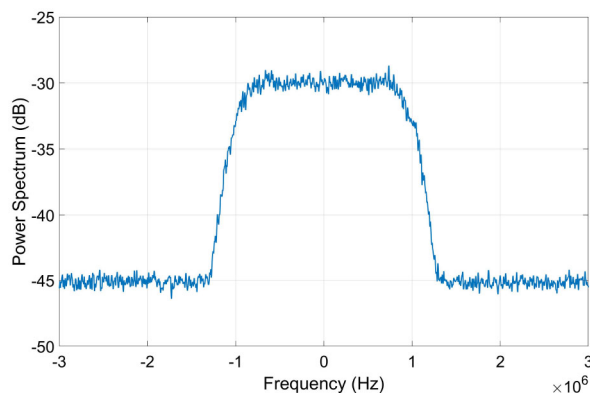
FIGURE 6. Validation. Spectrum of QPSK signal.

C. SYSTEM VALIDATION

The process of system validation plays a crucial part in the generation of appropriate QPSK symbols for the purpose of baseline evaluation. The validation process encompasses several essential steps.

First, the validation of the QPSK symbols generated in the simulation is performed by comparing their constellation diagram with the anticipated theoretical pattern as illustrated i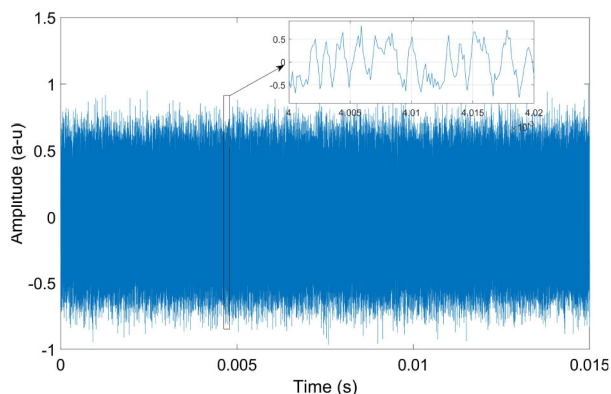n Fig. 4. The purpose of this visual comparison is to verify that the simulated symbols are in accordance with the expected QPSK modulation scheme.

Then, we check the waveforms in the time domain (Fig. 5) and the signal spectrum (Fig. 6) to verify the baseline system operation within the anticipated frequency range without any added interference.

The validation process serves to confirm that the simulation effectively represents the behavior of the QPSK radio connection in the absence of intentional interference.

It is possible to see different patterns in the complex plane when you look at the constellation diagrams for 16-PSK, 32-PSK, and 64-PSK modulation schemes. We sampled all these schemes at a fixed rate of 2 MHz and operated with a high SNIR of 25 dB for clearer constellation diagrams. In 16-PSK, there is a constellation of 16 points that are evenly spaced, as shown in Fig. 7. Each point represents a different phase shift, which in turn corresponds to 4 bits of data. Both the 32-PSK (Fig. 8) and 64-PSK (Fig. 9) constellations have 32 and 64 points, respectively, structured in a circle. Each point corresponds to a particular symbol. Even though higher-order modulations can be quite complex, all constellations have the expected pattern. These constellation diagrams display the signal space and phase changes between symbols. They show how PSK modulation can handle high data rates and reliable performance in noisy environments.
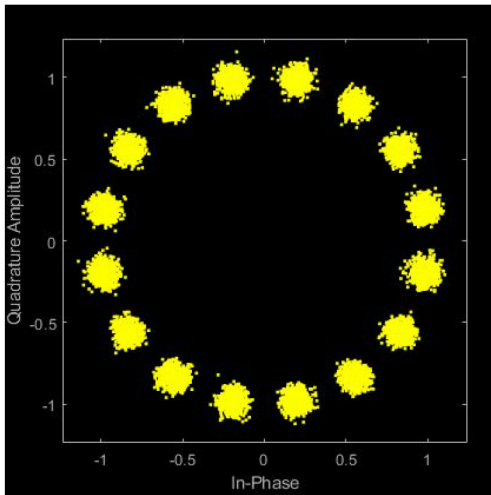
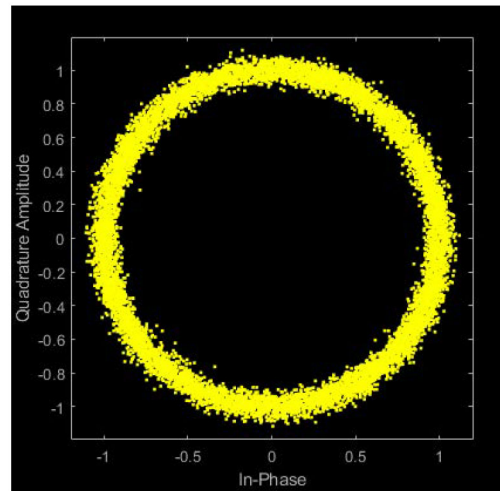**FIGURE 7.** 16-PSK constellation diagram symbols showed an SNIR power level of 25 dB at 2 MHz symbol rate.

FIGURE 9. 64-PSK constellation diagram symbols showed an SNIR power level of 25 dB at 2 MHz symbol rate.
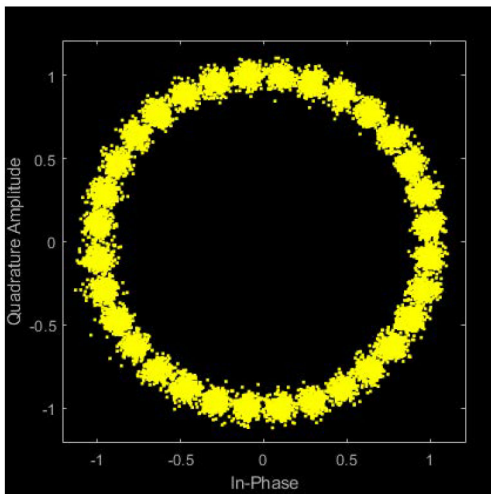

FIGURE 8. 32-PSK constellation diagram symbols showed an SNIR power level of 25 dB at 2 MHz symbol rate.

Making use of 16-PSK, 32-PSK, and 64-PSK can potentially enhance the data rate by encoding more bits per symbol. However, as the number of phases increases, the distance between symbols becomes smaller, making the system more sensitive to noise and interference. This can result in increased BER in practical communication links.

IV. RESULTS AND DISCUSSION

A. RESILIENCE UNDER CW EMI

The MATLAB simulation that injects CW with different frequencies (500 kHz in-band and 2 MHz out-of-band) into a baseband QPSK radio link shows the spectrum of the baseband signal in both time and frequency domains.

The baseband signal in the time domain represents the modulation of QPSK data onto the carrier frequency as illustrated in Fig. 10. When a 500 kHz CW disturbance is introduced into the in-band frequency range as shown in Fig. 11, it is contained within the baseband bandwidth and

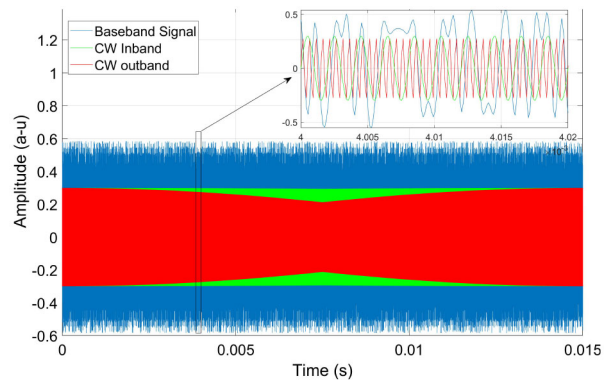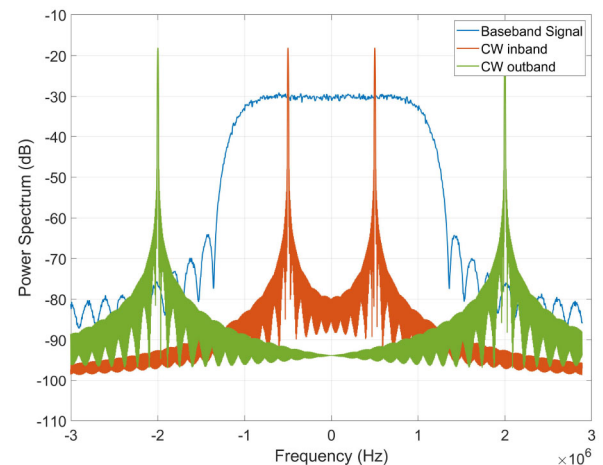**FIGURE 10.** QPSK radio link waveform with in- and out-band CW EMI.

FIGURE 11. QPSK radio link spectrum with in- and out-band CW EMI.

causes interference. The presence of interference can alter amplitude and phase, resulting in waveform distortions and the possibility of symbol detection errors. As a consequence, interference may cause the waveform of the baseband signal to deviate from the ideal one.
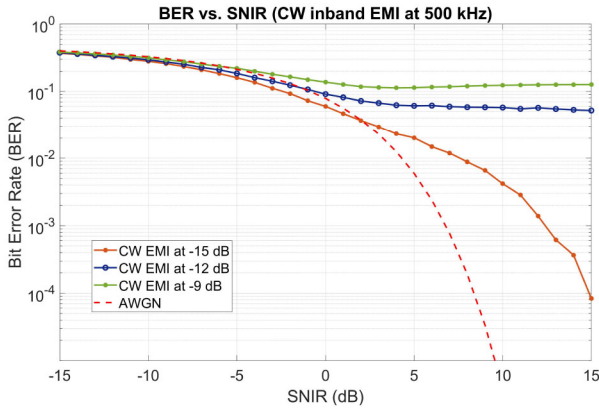
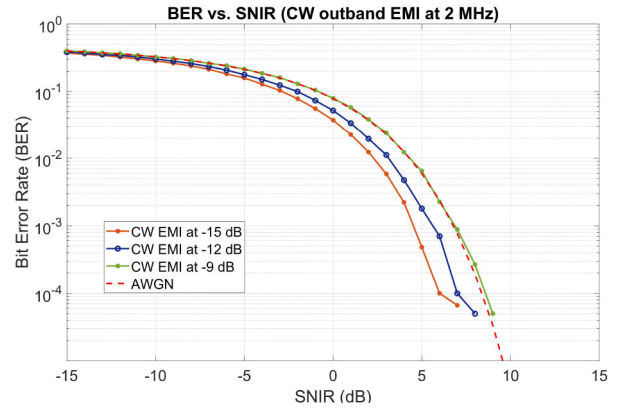**FIGURE 12.** QPSK radio link under in-band CW EMI at 500 kHz.

FIGURE 13. QPSK radio link under out-band CW EMI at 2 MHz.

We identified the parameter values in Table 1 through extensive simulation, using the method of trial and error to find the optimal settings for the simulation purposes. We made our decisions by analyzing performance metrics like BER and receiver sensitivity. We have also examined the potential limitations that may be associated with these choices to address interference in different conditions.

When an in-band perturbation at 500 kHz of CW is introduced, the spectrum plot in the frequency domain will show additional peaks around this frequency. The spectrum peaks represent interfering signals and their harmonics, indicating interference in the QPSK radio link baseband bandwidth. The occurrence of out-of-band disturbances results in spectral leakage, which has an impact on neighboring frequency segments inside the baseband bandwidth.

The plot of BER as a function of SNIR shows how the system performs at different SNIR levels and incorporates injected disturbances. We can examine disturbances on the QPSK link by adjusting the SNIR from -15 dB to 15 dB. One can assess the simulation's accuracy and dependability by comparing its results with the theoretical BER obtained using the *berawgn()* function.

The CW 500 kHz in-band interference has a detrimental impact on the quality of the received signal, resulting in errors during symbol detection and consequently leading to an elevated BER as illustrated in Fig. 12. Considering the bad SNIR, the impact of CW disturbance becomes more evident, leading to an increased BER. On the other hand, taking into account good SNIR leads to better performance in terms of lowering the BER levels.

However, the discrepancy between the BER due to exclusively AWGN theoretical BER and the simulated BER when CW out-of-band signals can be explained by multiple factors, such as signal processing techniques, levels of noise and interference, and the prevailing characteristics of the communication channel. The aforementioned factors have the potential to deviate from the assumptions that form the basis of the theoretical BER calculation.

Furthermore, a series of simulations were performed to evaluate the influence of the CW EMI peak power on communication links. In the first case, we varied the SNIR across a range of values, from "bad" to "good", while ensuring that the EMI level remained below the specified threshold (low impact) of -15 dB. The results highlight Fig. 13 that a lower level of EMI has a notable improvement in terms of BER, thereby enhancing the overall performance of the QPSK link. The observed behavior was noted through the addition of CW interference at the out-band frequencies. However, lower SNIR values below -5 dB are insufficient for the system to differentiate a signal from noise. Because the system struggles to recover the right information from the distorted signal, the BER is constant. As the SNIR rises over -5 dB, the signal becomes more distinct from noise and interference, improving performance and lowering BER.

A study [23] presents a partially comparable scenario of the same modulation, like QPSK, with different BER and SNIR values. Although they have applied single dominant synchronous co-channel interference to assess the performance, compared with the previous work, we have much-improved outcomes at lower SNIR values, as can be seen from Figs. 12 and 13, which exhibit satisfactory performance against both in-band and out-band scenarios of EMI.

In the second case, the SNIR remained unchanged, while the EMI level was intentionally set above the established threshold (high impact), specifically at -9 dB, in order to evaluate the effects at elevated levels. The findings suggest that the performance of out-band CW EMI was satisfactory, while the in-band CW EMI remained consistent after reaching a certain threshold of SNIR as shown in Fig. 12. The results indicate that the performance of the baseband QPSK radio link was significantly impaired by the presence of in-band CW interference at higher levels of EMI.

In the third case, we changed the CW EMI at -12 dB medium impact, while maintaining a constant SNIR. The purpose of this variation in EMI levels was to evaluate the efficiency of QPSK radio links under varying interference conditions. Results indicated that the QPSK radio links
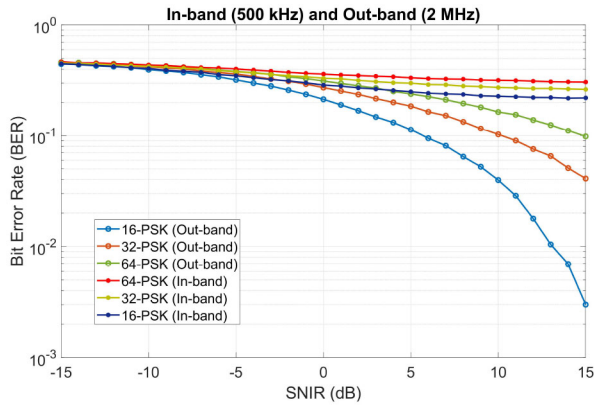
FIGURE 14. Receiver sensitivity curves for 16-PSK, 32-PSK and 64-PSK modulation schemes under CW EMI at 2 MHz symbol rate.

FIGURE 15. QPSK radio link baseband signal frequency domain with in- and out-band chirp EMI.

FIGURE 16. QPSK radio link baseband signal in time domain with in- and out-band chirp EMI.

exhibited satisfactory performance across all levels of varying EMI during the out-band CW interference, as illustrated in Fig. 13. It has been confirmed that beyond the desired frequency range, higher levels of EMI do not have a substantial effect, indicating greater resistance to external disturbances within that particular range. The aforementioned data emphasizes the significance of efficiently managing EMI levels and showcases the resilience of QPSK radio links in withstanding interference originating from frequencies outside the desired band. Only the out-of-band interference has less effect because it lies outside the baseband bandwidth of the radio link.

These results show how in-band and out-of-band CW interference affects the system performance for 16-PSK, 32-PSK, and 64-PSK modulation schemes at a symbol rate of 2 MHz. In-band CW interference, occurring within the baseband frequency of the signal, has a significant impact on the performance of modulation schemes, as shown in the results in Fig. 14. The presence of in-band interference makes it even more complicated for symbols to separate in higher-order PSK modulations, which increases the likelihood of errors occurring and results in a higher BER value. Conversely, out-of-band CW interference, occurring at frequencies outside the signal bandwidth, also contributes to system degradation, but to a lesser extent compared to in-band interference. Despite this, out-of-band interference still has some impact on the system performance by introducing additional noise and disrupting the reception of the signal. The receiver sensitivity curves clearly show the combined effect of both in-band and out-of-band CW interference. This shows how important it is to reduce interference sources and improve system parameters for secure communication in high-order PSK modulation schemes.

In contrast, when examining the identical scenario, it becomes evident that the presence of in-band CW interference significantly affects the effectiveness of QPSK radio links. The intensified level of interference has the potential to result in an increased BER and an impairment in signal quality. It can be observed from the results that the
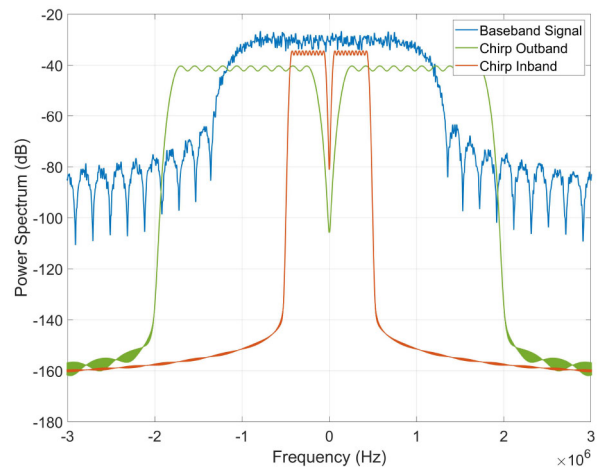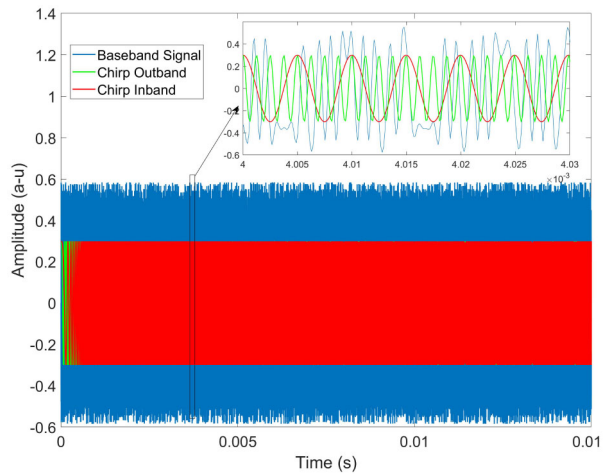
communication link tends to exhibit improved performance and lower BER values when subjected to lower EMI levels. Nevertheless, when the EMI surpasses specific thresholds, it can have a substantial impact on the performance of the communication link. This can lead to increased error rates and diminished reliability.

B. RESILIENCE UNDER CHIRP EMI

In this second scenario, the MATLAB simulation involves the injection of chirp interference with varying bandwidths (500 kHz and 2 MHz) in a baseband QPSK signal. The 500 kHz chirp sweeps completely inside the band while the 2 MHz chirps produce both in-band and out-band interference, therefore the impact of spectral leakage is also considered. Fig. 15 and Fig. 16 represent in time and frequency domain the chirp EMC along with the communication signal.

As demonstrated in Fig. 17 the presence of a chirp disturbance at the in-band frequency of 500 kHz has a

FIGURE 17. QPSK radio link under in-band chirp EMI at 500 kHz.

FIGURE 18. QPSK radio link under out-band chirp EMI at 2 MHz.

FIGURE 19. Receiver sensitivity curves for 16-PSK, 32-PSK and 64-PSK modulation schemes under Chirp EMI at 2 MHz symbol rate.

significant impact on system efficiency. This disturbance, which is characterized by continuous frequency variation, introduces various frequency components that can distort the received signal, resulting in symbol errors and a higher BE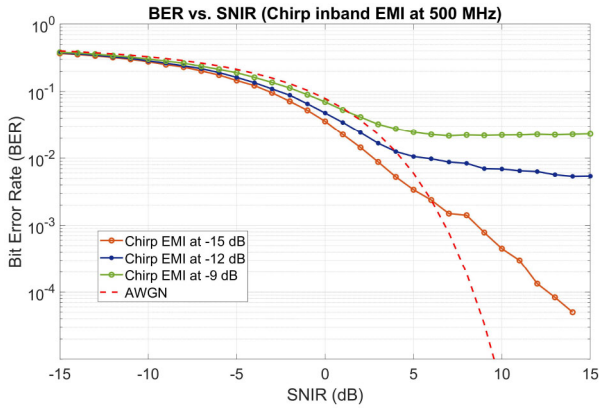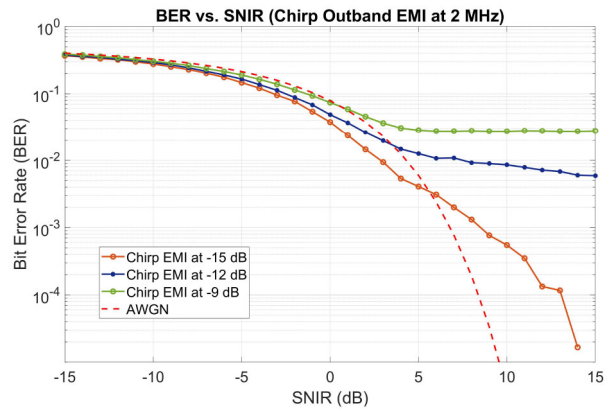R. This effect becomes more pronounced as the SNIR decreases. Introducing a chirp disturbance at 2 MHz, which is outside of the baseband bandwidth, can still affect BER performance. This is due to spectral leakage, which affects adjacent frequency bins within the baseband, potentially degrading the integrity of the QPSK signal and causing symbol detection errors. However, the magnitude of this effect varies with SNIR levels.

Additional simulations were undertaken to conduct a more comprehensive investigation into the effects of chirp EMI on the QPSK radio link. In the initial case, we varied the SNIR within a specific range of values, from "bad" to "good", while ensuring that the chirp EMI level remained below the predetermined threshold of -15 dB (low impact). Remarkably, the QPSK radio link exhibited a satisfactory level of robustness despite the presence of both in-band and out-of-band chirp interferences, which had minimal impact as demonstrated in Fig. 18. This outcome suggests that the QPSK radio link showcased robustness and sustained satisfactory performance despite the presence of chirp interference at the specified EMI levels.

In the second case, all other variables were identical except for the EMI level, which was increased to -9 dB, surpassing the established limit. The performance of the QPSK radio link did not significantly improve in either the in-band or out-of-band chirp interference scenarios. The only improvement observed was in the out-of-band chirp interference, resulting in a lower BER. For instance, once a specific SNIR threshold, such as 7 dB, the BER performance shows consistent behavior in both high-impact chirp EMI interference scenarios. The findings of this study indicate that once a specific threshold of SNIR is reached, there is no additional enhancements in BER were observed for the QPSK radio link under the chirp interferences.

In the third case, all other variables remained the same except the chirp EMI level of -12 dB medium impact. When
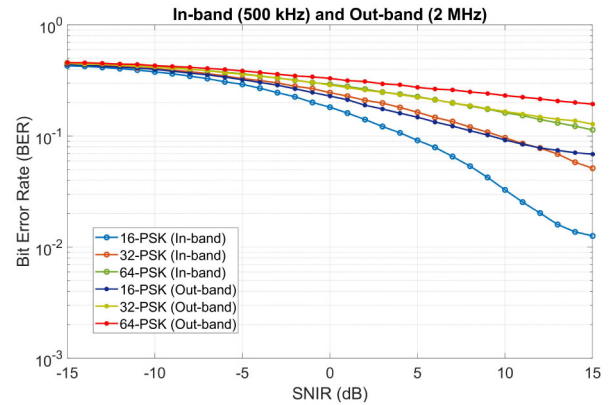
evaluating the situation involving in-band chirp interference, it was observed that the performance of the QPSK radio link was satisfactory only under conditions of low EMI levels. Nevertheless, it can be observed from Fig. 17 that the performance remained consistent despite the increase in EMI level. Conversely, in the context of out-of-band chirp interference, the QPSK radio link demonstrated not much-improved performance and efficiency. However, when examining higher levels of EMI, the noticed enhancement was minimal, as illustrated in Fig. 18. The findings indicate that the QPSK radio link exhibited average performance when subjected to out-of-band chirp interference. In contrast, the in-band scenario demonstrated satisfactory performance merely at lower EMI levels. This emphasizes the significance of EMI levels in influencing the effectiveness of the link in both interference scenarios.

We can see that in-band chirp interference has a bigger impact on receiver sensitivity when we use higher-order PSK modulation schemes like 16-PSK, 32-PSK, and 64-PSK (Fig. 19). This is because the effects of higher modulation orders are stronger. Chirp interference poses a significant concern in communication links, especially in higher-order PSK schemes because they have more closely packed constellation points. As the modulation order increases, the symbols in the constellation become closer together.

This reduces the margin for error and makes the system more vulnerable to interference. In this scenario, chirping within the signal bandwidth significantly impacts the system's performance more than chirping outside the signal bandwidth. The closer together the constellation points are, the more the interference from in-band chirping intensifies. This leads to more errors in the transmission of bits and a decrease in the overall system reliability. The results show that if you want to keep communication working well, especially in higher-order PSK modulation schemes with closely spaced symbols, you need to deal with in-band chirp interference. Therefore, it is crucial to identify optimal methods for reducing interference and adjusting system settings to ensure effective communication during chirp interference, particularly in the context of higher-order PSK modulation.

Adding an adaptive feature to PSK modulation can greatly reduce interference by changing the modulation scheme based on the current channel conditions. This adaptive approach improves communication resiliency by selecting the most appropriate modulation scheme for the current environment, effectively minimizing interference at each level. The adaptive system intelligently changes between different PSK modulation orders by constantly checking things like SNIR levels. This improves performance and reduces errors. This adaptive feature allows the optimal use of the available bandwidth and maximizes data throughput while ensuring reliable communication in challenging conditions.

C. EVM METRICS FOR CW AND CHIRP EMI RESILIENCE

A MATLAB simulation using EVM metrics assesses the baseband QPSK radio link in this study. CW and chirp electromagnetic disturbances at 500 kHz in-band and 2 MHz out-of-band are introduced into the simulation. The EVM simulation findings provide valuable insights into QPSK radio link performance analysis under these interferences. Key measures including RMS EVM, Max EVM, Percentile EVM, and EVM (in decibels) help assess QPSK radio link quality.

This work demonstrates the effects of proposed interferences on the modulation quality of the QPSK radio link through the presentation of EVM results. Table 2 presents quantifiable measures of degradation caused by these disturbances are represented by the specific values of RMS EVM, Max EVM, Percentile EVM, and EVM (dB), considering the SNIR bet at 15 dB. The findings assist in determining the extent of distortion and possible symbol errors caused by interferences, facilitating an evaluation of the modulation quality and overall effectiveness of the QPSK radio connection under various interference scenarios. This work gives a thorough explanation and analysis of the EVM results that assist in getting a better idea of how narrowband and broadband interferences affect radio quality. It is imperative to understand the significance of the findings and the capacity to assess and measure the decline in the

TABLE 2. Performance of the baseband QPSK link in terms of the EVM.

EMI source	EVM_{RMS}	EVM_{MAX}	$EVM_\%$	EVM(dB)
CW EMI at 500 kHz	10.91	53.19	0.0138	-19.24
CW EMI at 2 MHz	0	0	0.0130	0
Chirp EMI at 500 kHz	8.90	54.31	0.013	-21.01
Chirp EMI at 2 MHz	4.86	53.47	0.012	-26.26

performance of the QPSK radio link due to CW and chirp interferences.

The occurrence of in-band chirp disturbance results in a much BER when compared to CW disturbance. The introduction of out-of-band chirp disruption results in interference that has a negligible impact on the BER. In order to maintain consistent and dependable communication in the presence of fluctuating SNIR levels, the implementation of appropriate interference mitigation techniques, including adaptive filtering, equalization, and frequency hopping, becomes crucial. The QPSK radio connection demonstrates superior performance in the face of CW interference. This is evident from the EVM assessment presented in Table 2, which indicates that the signal quality is preserved and interference within the communication band is minimized.

V. CONCLUSION

This paper presents a thorough evaluation of QPSK radio links subject to CW and chirp interferences. The analysis of in-band and out-of-band interference scenarios improves our comprehension of the performance of baseband radio links. The results demonstrate that QPSK radio links operate better in the face of CW interference than chirp interference. These insights facilitate the improvement of digital communication links, ensuring their robustness and reliability in the presence of interferences. The evaluation assessed the efficiency of the QPSK radio link using key performance metrics such as the BER and EVM. By thoroughly adjusting noise power and receiver delay, the baseband communication links BER performance was enhanced to meet radio link requirements. However, more improvements are required to reduce the impact of chirp in-band interference. The assessment also revealed a significant decrease in RMS EVM during the transition from chirp interference to CW disturbance, indicating as 10.91 to 8.90 an improvement in the performance of the QPSK radio link. Undoubtedly, chirp interference has a greater negative impact on radio link evaluation than CW disturbance. The results provide insights for improving radio link performance under in-band and chirp EMI scenarios. Further improvements are required to reduce these interferences influence on higher-order PSK modulation. Further lines of work can be carried out for the optimization and parameter tuning of the QPSK radio link in the face of in-band CW EMI and chirp interference.

REFERENCES

[1] M. Li and G. Wei, "A review of quantitative evaluation of electromagnetic environmental effects: Research progress and trend analysis," *Sensors*, vol. 23, no. 9, p. 4257, 2023.

[2] P. F. Stenumgaard, "On radiated emission limits for pulsed interference to protect modern digital wireless communication systems," *IEEE Trans. Electromagn. Compat.*, vol. 49, no. 4, pp. 931–936, Nov. 2007.

[3] L. Rejfek, P. Rozsival, T. Zalabsky, T. N. Nguyen, P. T. Tran, and V. Stejskal, "Resistance of the radio modems against the narrow band interference," in *Proc. 33rd Int. Conf. Radioelektronika (RADIOELEKTRONIKA)*, 2023, pp. 1–4.

[4] M. Pous, M. A. Azpúrua, and F. Silva, "Measurement and evaluation techniques to estimate the degradation produced by the radiated transients interference to the GSM system," *IEEE Trans. Electromagn. Compat.*, vol. 57, no. 6, pp. 1382–1390, Dec. 2015.

[5] M. Pous and F. Silva, "Prediction of the impact of transient disturbances in real-time digital wireless communication systems," *IEEE Electromagn. Compat. Mag.*, vol. 3, no. 3, pp. 76–83, 3rd Quarter., 2014.

[6] M. A. Hannan, S. M. Abbas, S. A. Samad, and A. Hussain, "Modulation techniques for biomedical implanted devices and their challenges," *Sensors*, vol. 12, no. 1, pp. 297–319, 2012.

[7] K.-H. Teng and C.-H. Heng, "A 370-pJ/b multichannel BFSK/QPSK transmitter using injection-locked fractional-N synthesizer for wireless biotelemetry devices," *IEEE J. Solid-State Circuits*, vol. 52, no. 3, pp. 867–880, Mar. 2017.

[8] H.-C. Chen and W.-K. Lee, "Battery-less ASK/O-QPSK transmitter for medical implants," *Electron. Lett.*, vol. 48, pp. 1036–1038, Aug. 2012.

[9] D. Li, Y. Zhou, S. Chen, and X. Xu, "A quasi-digital QPSK modulator design for biomedical devices," *Assoc. Comput. Mach.*, vol. 18, no. 2, pp. 1–16, Apr. 2022. [Online]. Available: https://doi.org/10.1145/3465379

[10] P. Stenumgaard and K. Wiklundh, "An improved method to estimate the impact on digital radio receiver performance of radiated electromagnetic disturbances," *IEEE Trans. Electromagn. Compat.*, vol. 42, no. 2, pp. 233–239, May 2000.

[11] M. Pous, M. A. Azpúrua, and F. Silva, "Radiated transient interferences measurement procedure to evaluate digital communication systems," in *Proc. IEEE Int. Symp. Electromagn. Compat. (EMC)*, 2015, pp. 456–461.

[12] L. Yuan, J. Zhang, Z. Liang, M. Hu, G. Chen, and W. Lu, "EMI challenges in modern power electronic-based converters: Recent advances and mitigation techniques," *Front. Electron.*, vol. 4, Nov. 2023, Art. no. 1274258.

[13] W. El Sayed, P. Crovetti, N. Moonen, P. Lezynski, R. Smolenski, and F. Leferink, "Electromagnetic interference of spread-spectrum modulated power converters in G3-PLC power line communication systems," *IEEE Lett. Electromagn. Compat. Pract. Appl.*, vol. 3, no. 4, pp. 118–122, Dec. 2021.

[14] A. T. Balaei, A. G. Dempster, and L. L. Presti, "Characterization of the effects of CW and pulse CW interference on the GPS signal quality," *IEEE Trans. Aerosp. Electron. Syst.*, vol. 45, no. 4, pp. 1418–1431, Oct. 2009.

[15] X. Huang, Y. Chen, and Y. Wang, "Simulation of interference effects of UWB pulse signal to the GPS receiver," *Discr. Dyn. Nat. Soc.*, vol. 2021, pp. 1–8, Jul. 2021. [Online]. Available: https://www.hindawi.com/journals/ddns/2021/9935543/

[16] L. S. Rojas. "Simulated assessment of interference effects in direct sequence spread spectrum (DSSS) QPSK receiver." 2014. [Online]. Available: https://scholar.afit.edu/etd/620.

[17] B. Çiftçi, J. Gross, T. Augustin, X. Wang, S. Norrga, and H.-P. Nee, "Wireless communication in modular multilevel converters and electromagnetic interference Characterization," *IEEE Access*, vol. 10, pp. 38189–38201, 2022.

[18] T. Xu, M. Zhao, and Y. Chen, "Study on continuous wave electromagnetic interference effect of UAV data link," in *Proc. 13th Glob. Symp. Millim.-Waves Terahertz (GSMM)*, 2021, pp. 1–3.

[19] X. Ouyang and J. Zhao, "Orthogonal chirp division multiplexing for coherent optical fiber communications," *J. Lightw. Technol.*, vol. 34, no. 18, pp. 4376–4386, Sep. 2016.

[20] Z. Qu, J. Yang, and J. Chen, "Continuous wave interference effects on ranging performance of spread spectrum receivers," *Wireless Pers. Commun.*, vol. 82, pp. 473–494, May 2015.

[21] A. E. Pena-Quintal, M. J. Basford, K. Niewiadomski, S. Greedy, M. Sumner, and D. W. P. Thomas, "Data links modelling under radiated EMI and its impact on sampling errors in the physical layer," in *Proc. Int. Symp. Electromagn. Compat. (EMC EUROPE)*, 2020, pp. 1–5.

[22] K. V. C. Aadal. "Chirp spread spectrum RTLS, location tracking, & positioning." 2022. Accessed: Jul. 21, 2022. [Online]. Available: https://www.inpixon.com/technology/standards/chirp-spread-spectrum

[23] C. Ball, E. Humburg, and F. Treml, "Different OFDM link level performance under the presence of co-channel interference and noise," in *Proc. IEEE 17th Int. Symp. Pers., Indoor Mobile Radio Commun.*, 2006, pp. 1–6.

ASIF ALI received the B.E. degree in telecommunication engineering and the M.Eng. degree in telecommunication engineering and management from the Mehran University of Engineering and Technology, Jamshoro, Pakistan, in 2017 and 2020, respectively. He is currently pursuing the Ph.D. degree in electronic engineering with Universitat Politècnica de Catalunya, Barcelona, Spain, as part of the Marie Skłodowska-Curie Innovative Training Network Project Eternity. His current research interests include the modeling and evaluation of electromagnetic interference on digital communication systems and EMI-resilient links for medical devices.

MIREYA FERNÁNDEZ CHIMENO received the degree in telecommunications engineering and the Ph.D. degree from Universitat Politècnica de Catalunya (UPC), Spain, in 1990 and 1996, respectively.

Since 1998, she is an Associate Professor with Electronic Engineering Department, UPC. She belongs to the Biomedical and Electronic Instrumentation Group where she developed her research with the Grup of Electromagnetic Compatibility where she is a Quality Manager, and the Center for Research of Biomedical Engineering, both centers part of the TECNIO network of the Generalitat de Catalunya. She was the Deputy Director of teaching laboratories with the School of Telecommunications Engineering ETSETB, UPC, from 1996 to 2000 and a Visiting Researcher with the Department of Health Sciences, York University in 2003. She was a Councilor of Gelida, Barcelona, from 2007 to 2011, overseeing new technology and community participation. She has co-authored over 100 scientific and academic articles, conference communications, and books and 7 patents. EMC Europe 2006 Barcelona and EMC Europe 2019 Barcelona organizing committees, the Biodevices 2013 Program Chair, the Biodevices / Biostec Program Committee Member since 2013, and the Phycs Member since 2017.

MARCO A. AZPÚRUA (Senior Member, IEEE) received the B.Sc. degree in telecommunications and the M.Sc. degree in electrical engineering from the Universidad Central de Venezuela in 2008 and 2013, respectively, and the Ph.D. degree in electronics engineering from the Universitat Politècnica de Catalunya (UPC), Spain, in 2018 for its contributions to Full Time-Domain EMI measurements and their applications. He is currently works as an Associate Professor with the Electronic Engineering Department, UPC, where he is a part of the EMC Group. He was a recipient of the IEEE Instrumentation and Measurement Society Faculty Course Development Award in 2020, the UPC Special Doctoral Award for the Best Thesis in the field of Electronics, and the Best Student Paper Award in the 2017 EMC Europe. He is the Co-founder of EMC Barcelona, a Fellow of the StandICT.eu 2023 Project and a member of the CISPR/CIS/B/WG 1 & WG 7, the IEEE TRANSACTIONS ON ELECTROMAGNETIC COMPATIBILITY and IMS societies, and the IEEE/ICES.